Redox Biology 36 (2020) 101682

Contents lists available at ScienceDirect

Redox Biology

journal homepage: www.elsevier.com/locate/redox

Research Paper

The cholesterol metabolite 27-hydroxycholesterol inhibits SARS-CoV-2 and is markedly decreased in COVID-19 patients

Alessandro Marcello [a,1], Andrea Civra [b,1], Rafaela Milan Bonotto [a], Lais Nascimento Alves [a], Sreejith Rajasekharan [a], Chiara Giacobone [c], Claudio Caccia [d], Roberta Cavalli [e], Marco Adami [f], Paolo Brambilla [c], David Lembo [b,**], Giuseppe Poli [g,*,2], Valerio Leoni [c]

[a] Laboratory of Molecular Virology, International Centre for Genetic Engineering and Biotechnology (ICGEB), Trieste, 34149, Italy
[b] Laboratory of Molecular Virology and Antiviral Research, Department of Clinical and Biological Sciences, University of Turin, San Luigi Hospital, Orbassano, Turin, 10043, Italy
[c] Laboratory of Clinical Chemistry, Hospitals of Desio and Monza, ASST-Monza and Department of Medicine and Surgery, University of Milano-Bicocca, Monza, 20900, Italy
[d] Unit of Medical Genetics and Neurogenetics, Fondazione IRCCS Istituto Neurologico Carlo Besta, Milan, 20133, Italy
[e] Department of Drug Science and Technology, University of Turin, Turin, Italy
[f] Department of Pharmacological and Biomolecular Sciences, University of Milan, 20133, Italy
[g] Unit of General Pathology and Physiopathology, Department of Clinical and Biological Sciences, University of Turin, San Luigi Hospital, Orbassano, Turin, 10043, Italy

ARTICLE INFO

Keywords:
Coronavirus
SARS-CoV-2
COVID-19
HCoV-OC43
Cholesterol
Oxysterols
27-Hydroxycholesterol

ABSTRACT

There is an urgent need to identify antivirals against the coronavirus SARS-CoV-2 in the current COVID-19 pandemic and to contain future similar emergencies early on. Specific side-chain cholesterol oxidation products of the oxysterols family have been shown to inhibit a large variety of both enveloped and non-enveloped human viral pathogens. Here we report on the in vitro inhibitory activity of the redox active oxysterol 27-hydroxycholesterol against SARS-CoV-2 and against one of the common cold agents HCoV-OC43 human coronavirus without significant cytotoxicity. Interestingly, physiological serum levels of 27-hydroxycholesterol in SARS-CoV-2 positive subjects were significantly decreased compared to the matched control group, reaching a marked 50% reduction in severe COVID-19 cases. Moreover, no correlation at all was observed between 24-hydroxycholesterol and 25-hydroxycholesterol serum levels and the severity of the disease. Opposite to that of 27-hydroxycholesterol was the behaviour of two recognized markers of redox imbalance, i.e. 7-ketocholesterol and 7β-hydroxycholesterol, whose serum levels were significantly increased especially in severe COVID-19. The exogenous administration of 27-hydroxycholesterol may represent in the near future a valid antiviral strategy in the worsening of diseases caused by present and emerging coronaviruses.

1. Introduction

The present COVID-19 pandemic caused by the coronavirus SARS-CoV-2 is yet another example of the dramatic impact of emerging viral infections on human morbidity and mortality worldwide. Currently, no specific drug for the new coronavirus is available and repurposing is the only strategy in place [1]. Clearly, there is an urgent need for drugs active against a wider number of viruses to contain future emergencies early on. Host directed therapy aims at targeting essential host factors for viral replication and triggering immune antiviral pathways [2]. Advantages of this approach include not only the possibility of targeting multiple viruses, but also an increased threshold to the emergence of resistance.

Selective cholesterol oxidation products, of the oxysterol family, which are ligands of Liver X Receptors (LXRs), have a well-recognized immunomodulatory role [3,4]. Oxysterols such as 25-hydroxycholesterol (25OHC) have shown to markedly inhibit the replication of a large variety of both enveloped and non-enveloped human viral

* Corresponding author.
** Corresponding author.
E-mail addresses: david.lembo@unito.it (D. Lembo), giuseppe.poli@unito.it (G. Poli).
[1] Equally contributing to the work.
[2] Lead contact.

https://doi.org/10.1016/j.redox.2020.101682
Received 20 July 2020; Received in revised form 1 August 2020; Accepted 6 August 2020
Available online 10 August 2020

pathogens [5–7]. However, another oxysterol of enzymatic origin, namely 27-hydroxycholesterol (27OHC), is gaining increasing consideration as a protective molecule not only against the respiratory virus Rhinovirus, but also against a wide range of other viral infections [8–11]. There is clear evidence that exogenously added 27OHC accumulates in plasma membrane lipid rafts, likely affecting viral entry but also modulating cell signaling stemming from such microdomains [12,13].

Both 25OHC and 27OHC are side-chain oxysterols physiologically present in human peripheral blood, cerebrospinal fluid [14,15], colostrum and milk [16]. 27OHC is constitutively the most abundant oxysterol in these biological fluids and present in various tissues and organs, being synthesized by the ubiquitous mitochondrial enzyme 27-cholesterol hydroxylase (Cyp27A1) [15].

Due to the emerging role of 27OHC as a broad-spectrum antiviral, we deemed relevant to investigate whether it could inhibit SARS-CoV-2 and other coronaviruses. Here we report on the in vitro antiviral activity of 27OHC against SARS-CoV-2 and the human coronavirus HCoV-OC-43. Moreover, we analyzed the serum levels of 27OHC in 123 healthy individuals, in 27 pauci-or a-symptomatic SARS-CoV-2 positive subjects (PACP) and in 117 COVID-19 patients and found quite a marked decrease of the oxysterol in COVID-19 patients that correlates with the severity of the disease. Another notable finding was the increase of serum 7-ketocholesterol and 7 β-hydroxycholesterol, two reliable markers of tissue oxidative imbalance, in moderate and severe COVID-19 patients.

2. Methods

2.1. Reagents

The oxysterol 27OHC complexed with 2-hydroxypropyl-β-cyclodextrin (2HP-βCD:27OHC) was kindly provided by Panoxyvir Ltd (Turin, Italy). The *anti*-RSV monoclonal antibody Ab35958 was purchased from Abcam (Cambridge, United Kingdom). The secondary antibody peroxidase-conjugated AffiniPure F (ab')2 Fragment Goat Anti-Mouse IgG (H+L) was purchased from Jackson ImmunoResearch Laboratories Inc. (West Grove, PA, USA). The recombinant antibody mSIP-3022 against SARS-CoV-2 Spike was previously described [17].

2.2. Cell lines and viruses

Vero E6 cells (African green monkey kidney cells) (ATCC®-1586) and human hepatocarcinoma Huh7 cells kindly provided by Ralf Bartenschlager (University of Heidelberg, Germany) were cultured in DMEM (Gibco) supplemented with 10% fetal bovine serum (Gibco). Human lung fibroblast MRC-5 (ATCC® CCL-171) and human epithelial cells Hep-2 (ATCC® CCL-23) were propagated in Dulbecco's Modified Eagle Medium (DMEM; Sigma, St. Louis, MO, USA) supplemented with 1% (v/v) penicillin/streptomycin solution (Euroclone, Milan, Italy) and heat inactivated, 10% (v/v) fetal bovine serum (Sigma).

SARS-CoV-2 isolate ICGEB_FVG_S5 was obtained at ICGEB as previously described [18]. Plaque assay was performed by incubating dilutions of SARS-CoV-2 on Vero E6 monolayers at 37 °C for 1 h. These were then washed with phosphate buffered saline (PBS) and overlaid with DMEM 2% FBS containing 1.5% carboxymethylcellulose for 3 days. Cells were then fixed with 3.7% paraformaldehyde (PFA) and stained with crystal violet 1%.

Human coronavirus strain OC43 (HCoV–O43) (ATCC® VR-1558) was purchased from ATCC (American Type Culture Collection, Rockville, MD, USA) and propagated in MRC-5 cells, at 33 °C, in a humidified 5% CO2 incubator. When the full cytopathic effect (CPE) developed, cells and supernatants were harvested, pooled, frozen, and thawed three times, then clarified and aliquoted. The virus was stored at −70 °C. CoV titers were determined by the standard plaque method. Briefly, MRC-5 cells were seeded 2 days before infection in 96-well plates, reaching 60%–70% confluence at the time of infection. The viral suspension was serially diluted in DMEM supplemented with 2% fetal bovine serum and inoculated; the infected wells were incubated at 33 °C for 1 h, allowing viruses to attach and enter the cells. After this time, cells were washed with medium, and overlaid with a 1:1 combination of 1.6% SeaPlaque Agarose (BioWhittaker Molecular Applications) and 2 × DMEM medium (Gibco BRL) as described elsewhere [8]. The plates were incubated at 33 °C for 3 days. After incubation, the plates were fixed and stained as described elsewhere [8], and the number of plaques formed was counted; viral titers were expressed in terms of plaque forming units per ml (PFU/ml). Respiratory syncytial virus (RSV) strain A2 (ATCC VR-1540) was propagated in Hep-2 and titrated by the indirect immunoperoxidase staining procedure as described elsewhere [19]. Viral titers were expressed as focus-forming unit (FFU) per ml. Viruses were stored at −80 °C.

2.3. COVID-19 patients and control individuals

We consecutively included in this study 144 adults with SARS-CoV-2 infection confirmed through real-time reverse-transcriptase–polymerase-chain-reaction (RT-PCR) assays of nasal and pharyngeal swabs, in accordance with WHO guidance [20–22]. RT-PCR was performed at San Gerardo Hospital, Monza, and subsequently at the Italian National Institute of Health, Rome, Italy.

Of them, 117 were COVID-19 patients hospitalized from March 2020 at Desio Hospital, ASST-Monza, Italy: 36 had moderate disease presentation (F:M = 13:23, age 65.5 ± 13.5 years, median = 67.12, IQR = 58.6–77.3, min-max range = 32.59–87.48) and 81 had severe disease presentation (F:M = 15:66, age = 69.73 ± 12.99, median = 72.38, IQR = 61.01–79.98, min-max = 33.68–92.27). All were sampled within 10 days from diagnosis (average: 2 days). Subjects were classified as severe if they presented one or more of the following symptoms: respiratory rate (RR) ≥ 30 breaths/min, finger oxygen saturation (SpO2) ≤ 93% at rest, and arterial partial pressure of oxygen (PaO2)/fraction of inspired oxygen (FIO2) ≤ 300 ratio [23,24]. The remaining 27 recruited subjects were SARS-CoV-2 positive patients with mild or minimal symptoms (PACP) not requiring hospitalization (age = 53.48 ± 6.43, median = 54.99, IQR = 47.75–59.15, min-max = 40.56–61.21). Controls were 123 apparently healthy individuals (F:M = 58:65, age = 68.22 ± 9.17, median = 65.46, IQR = 60.1–75.83, min-max = 57–89.99) collected at Desio Hospital before the pandemic outbreak.

2.4. Data collection

Basic information such as age, gender, comorbidities, clinical and laboratory data, chest radiograph (when performed), and outcome (survival or non-survival) was obtained from the electronic medical records of each patient and stored by a password-protected database.

2.5. Antiviral assays

The antiviral activity was determined by the plaque reduction assay. For SARS-CoV-2 experiments, Vero E6 cells were seeded in a 48 well plate, at 6×10^4 cells/well density and incubated at 37 °C overnight. For HCoV-OC43 and RSV, MRC-5 or Hep-2 cells, respectively were first seeded (at 2×10^4 cells/well) in 96 well plates and incubated at 37 °C overnight. The medium was removed from the plates and infection was performed respectively with 10–20 viral PFU per well of SARS-CoV-2 at 37 °C for 1 h, ca. 30 PFU of a stock of HCoV-OC43 at 33 °C for 1 h or ca. 30 PFU of RSV at 37 °C for 3 h, allowing the viruses to attach and enter the cells. After incubation, cells were washed with medium, and overlaid with medium containing 1% carboxymethylcellulose (CMC) with DMEM + 2% FBS, and compound dilutions for SARS-CoV-2 experiments, or with a 1:1 combination of 1.6% SeaPlaque Agarose and 2 × DMEM supplemented with different concentrations of compounds. After 72 h of incubation (33 °C, 5% CO2 for HCoV-OC43 or 37 °C, 5% CO2 for SARS-

CoV-2 and RSV), the medium with oxysterols was removed, and the plates were fixed with 3.7% paraformaldehyde (PFA) or 7.5% formaldehyde (Fluka) and stained with crystal violet (Sigma, St. Louis, Mo.). The number of plaques formed was counted. The plaque reduction assays were conducted in 2× replicate in two independent experiments. Blockade of viral infectivity was expressed as mean % ± standard error of the mean (SEM). Where possible, half-maximal antiviral effective concentration (EC_{50}) values were calculated by regression analysis using the dose-response curves generated from the experimental data using GraphPad PRISM 7 (GraphPad Software, San Diego, CA, USA). EC_{50} values were compared using the sum-of-squares F test.

2.6. Virus inactivation assay

Approximately 10^5 PFU of HCoV-OC43 were incubated with a concentration of 2HP-βCD:27OHC corresponding to EC_{90} in the antiviral assay. The HCoV-OC43/2HP-βCD:27OHC mixture was incubated for 1 h at 33 °C. A control experiment by treating the viral suspension with the blank formulation (2HP-βCD) was also performed. After the incubation, both treated and untreated viruses were titrated to the non-inhibitory concentration of 2HP-βCD:27OHC and the residual viral infectivity was determined by plaque counting. Statistical analysis was performed using One-Way Analysis of Variance (ANOVA), followed by Bonferroni post-hoc test. Significance was reported for p-value <0.05.

2.7. In vitro cytotoxicity assay

The cytotoxicity assay was conducted with Alamar Blue (Invitrogen) as recommended by the manufacturer's protocol. Vero E6 cells were seeded at 1×10^4 cells per well in a 96 well plate, and incubated at 37 °C overnight. Then 50 μL of compounds at the indicated concentrations were added to 150 μL of medium (final 200 μL). Plates were incubated at 37 °C for 3 days and then the colorimetric reagent was added (20 μL for 4 h). Measurements from compound-treated or vehicle-treated cells were normalized against those from untreated cells. The half maximum cytotoxic concentration (CC50) was calculated using GraphPad Prism Version 7. Cytotoxicity assay fluorescence readings were normalized for vehicle and percent plotted against dilutions expressed as antilog.

2.8. Cell viability assay

MRC-5 or Hep-2 cells were seeded at a density of 5×10^3/well in 96-well plates and treated the next day with 27OHC, 2HP-βCD:27OHC, or blank formulation at concentrations ranging from 0.07 to 150 μM to generate dose-response curves. Control samples (100% of viability) were prepared by treating cells with culture medium. After 72 h of incubation, cell viability was determined using a Cell Titer 96 Proliferation Assay Kit (Promega, Madison, WI, USA) and following the manufacturer's instructions. Absorbance was measured using a Microplate Reader (Model 680, Bio-Rad Laboratories, Hercules, CA, USA) at 490 nm. Viability of oxysterol-treated cells is expressed as a percentage relative to cells incubated with culture medium supplemented with equal volumes of ethanol.

2.9. Immunofluorescence

For SARS-CoV-2 analysis Huh7 cells were seeded on coverslips and infected with SARS-CoV-2 the following day at a multiplicity of infection (m.o.i.) of 0.1 PFU/cell. After 1 h, inoculum was removed and fresh DMEM +2% FBS containing 2HP-βCD:27OHC or 2HP-βCD was added to the cells. After 48 h incubation, cells were fixed with 3.7% PFA, treated with 100 mM glycine and 0.1% Triton X-100, with intermediate washes with PBS. A blocking step was performed at 37 °C for 30 min with 1% bovine serum albumin (BSA) and 0.1% Tween in PBS (blocking solution). The coverslips were then probed with the mSIP-3022 anti-Spike recombinant antibody diluted 1/200 with blocking solution and incubated overnight at 4 °C in humidified container. The reaction was completed by incubating fixed cells with polyclonal anti-mouse antibody conjugated with Alexa Fluor 594 (Molecular Probes, Oregon, USA) diluted 1/500 for 1 h at 37 °C. Coverslips were finally washed and mounted on glass slides using Fluoro-Gel II mounting medium with DAPI (Electron Microscopy Sciences, Pennsylvania, USA) and analyzed with a Zeiss LSM880 confocal microscope. For statistical purposes, 200 ± 10 cells were counted for each condition.

2.10. Clinical laboratory measurements

All clinical laboratory measurements were performed in the course of hospitalization. Count blood cells was performed on whole blood with K3-EDTA vacuum tubes and obtained by Sysmex XN-9000 platform (Sysmex, Germany). Blood chemistries were performed on serum vacuum tubes using COBAS 8000 platform (Roche Diagnostics, Germany).

2.11. Sterols and oxysterols quantification by isotope dilution GC-MS

To a screw-capped vial sealed with a Teflon septum, 0.25 mL of plasma were added together with 500 ng of D7-lathosterol, 50 ng of D6-lanosterol, 50 ng of D7-24S-hydroxycholesterol, 50 ng of D6-25-hydroxycholesterol, 50 ng of D6-27-hydroxycholesterol, 50 ng of D7-7-ketocholesterol, 50 ng of D7-7β-hydroxycholesterol (Avanti Polar Lipids), as internal standards, 50 μl of butylated hydroxytoluene (5 g/L) and 50 μl of K3-EDTA (10 g/L) to prevent auto-oxidation. Each vial was flushed with argon for 10 min to remove air. Alkaline hydrolysis was allowed to proceed at room temperature with magnetic stirring for 60 min in the presence of ethanolic 2 M potassium hydroxide solution. After hydrolysis, the sterols were extracted twice with 5 ml hexane. The organic solvents were evaporated under a gentle stream of argon and converted into trimethylsilyl ethers with BSTFA.

Gas chromatography mass spectrometry (GC-MS) analysis was performed on a GC equipped with an Elite column (30 m × 0.32 mmid × 0.25 mm film; PerkinElmer, USA) and injection was performed in splitless mode and using helium (1 ml/min) as a carrier gas. The temperature program was as follows: initial temperature of 180 °C was held for 1 min, followed by a linear ramp of 20 °C/min to 270 °C, and then a linear ramp of 5 °C/min to 290 °C, which was held for 10 min. The mass spectrometer operated in the selected ion-monitoring mode. Peak integration was performed manually, and sterols were quantified from selected-ion monitoring analysis against internal standards using standard curves for the listed sterols. Additional qualifier (characteristic fragment ions) ions were used for structural identification.

Inter-assay CV ranged between 2.3% for lathosterol and 5.3% for 25-hydroxycholesterol. Recovery ranged from 97 up to 104% (5–7).

2.12. Statistical analyses

Continuous variables were expressed as mean ± SD, median, interquartile ranges (IQR), min-max range and compared with the ANOVA or Mann-Whitney *U* test when non parametric distributed.

2.13. Ethics

The study was approved by the Ethical Committee of the Istituto Nazionale Malattie Infettive Lazzaro Spallanzani, Roma and stemmed as a sub-project of the Observational cohort study on the natural history of hospitalized SARS-CoV-2 patients: the STORM trial of the University of Milano Bicocca, Milan, Italy.

3. Results

3.1. 2HP-βCD:27OHC is endowed with antiviral activity against two pathogenic CoVs

The activity of 27OHC against SARS-CoV-2 and HCoV-OC43, was assessed on Vero-E6 and MRC-5 cells, respectively. To improve its solubility and stability, 27OHC was complexed with 2-hydroxypropyl-β-cyclodextrin, a carrier commonly used in drug formulations. Therefore, the complex (2HP-βCD:27OHC) and the carrier alone (2HP-βCD) were tested in parallel to rule out any contribution of the carrier to the antiviral activity.

As shown in Fig. 1 and Table 1, 2HP-βCD:27OHC, but not 2HP-βCD, exerted antiviral activity in a dose-response manner against both SARS-CoV-2 and HCoV-OC43 to maxima of inhibition of 100%, with EC_{50} values falling in the low micromolar range and with a favourable selectivity index (SI). Conversely, 2HP-βCD:27OHC did not inhibit the infectivity of RSV, an enveloped RNA virus also causing respiratory diseases, thus demonstrating that the antiviral specificity of 27OHC is broad but yet selective.

Time-of-addition experiments were then performed to investigate the step of viral replicative cycle inhibited by 2HP-βCD:27OHC. Two different conditions were used: briefly, cells were treated for 24 h before viral inoculum (pre-treatment protocol) or 3 h after inoculum (post-infection treatment protocol). 2HP-βCD:27OHC showed antiviral activity against the two CoVs both when it was added before and after inoculation (Fig. 2 and Table 2). However, the results show that 2HP-βCD:27OHC has greater efficacy against SARS-CoV-2 when added after infection, while it is more effective against HCoV-OC43 when added before inoculation. Furthermore, we investigated the ability of 2HP-βCD:27OHC to impair infectivity by directly targeting viral particles incubating HCoV-OC43 with 2HP-βCD:27OHC at high effective concentrations (EC_{90}) and then determining the viral titer at dilutions at which the treatment was no longer active when added on cells. As reported in Fig. S1, 2HP-βCD:27OHC was not able to inactivate HCoV-OC43 particles.

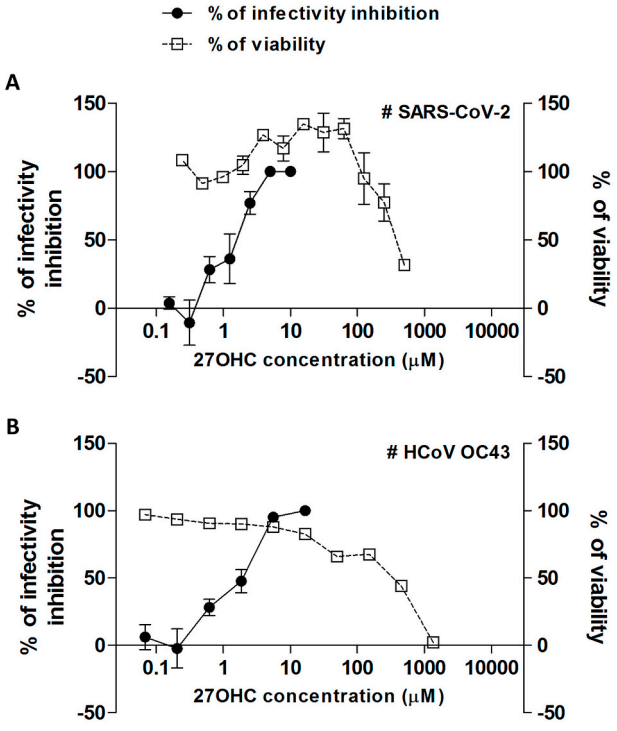

Fig. 1. Plaque reduction and cell viability assays. The antiviral activity of 2HP-βCD:27OHC was tested against SARS-CoV-2 (A) and HCoV OC43 (B), respectively on Vero-E6 cells and MRC-5 cells. Briefly, cells were infected for 1 h and treated for 72 h with increasing concentrations of 2HP-βCD:27OHC. Viral infections were detected as described in the Material and Methods section. Cell viability experiments were performed in the same conditions as for antiviral assays, in absence of viral inoculum. The percentage infectivity inhibition (black dots) and the percentage of cell viability (white squares) were calculated by comparing treated and untreated wells. Error bars represent the standard error of the mean (SEM) of 2 independent experiments.

The efficiency of SARS-CoV-2 and HCoV-OC43 infection was finally measured respectively in the human cell line Huh7 and MRC-5, in the presence of 2HP-βCD:27OHC. As shown in Fig. 3A and C, and quantified in Fig. 3B and D, 2HP-βCD:27OHC significantly ($p_{ANOVA} < 0.001$) reduced the number of infected cells 48 h post infection both at 3 μM and 20 μM. By contrast, 2HP-βCD failed to show any *anti*-CoV activity, showing no significant difference from the untreated control, in terms of number of infected cells.

3.2. Clinical laboratory parameters in moderate and severe COVID-19 patients

The in vitro evidence of effective inhibition of SARS-CoV-2 by the formulation 27OHC+2HP-βCD prompted us to carry on an observational cohort study in COVID-19 patients with the aim to monitor 27OHC serum content in the different stages of the disease. As detailed in the Methods section, the groups studied here were: 1) control, 2) pauci-asymptomatic SASR-CoV-2 positive individuals (PACP), 3) moderate COVID-19, 4) severe COVID-19. No age differences were observed between controls and COVID-19 patients, while the subjects of the pauci-asymptomatic group were significantly younger than all the other groups ($P < 0.001$ for all).

With regard to the standard laboratory parameters measured only in the hospitalized patients (see Table 3), HB and HCT, already below the normal values, were significantly lower in severe COVID-19 compared to moderate COVID-19 ($P = 0.04$ for both). Also serum creatinine was increased both in moderate and severe patients, being significantly higher in the severe COVID-19 group as compared to the moderate COVID-19 one ($P = 0.03$). Alanine Aminotransferase (ALT) and Lactate Dehydrogenase (LDH) were moderately above the normal range, while Creatine Kinase (CK) was much higher respect to the normal values, in all cases without significant difference between the two groups of patients. C Reactive Protein (CRP), resulted to be markedly elevated in COVID-19 with a tendency to increase in the severe cases, and Procalcitonin (PCT), a marker of sepsis, showed a net average increase in the severe COVID-19 group, that however did not reach statistical significance.

3.3. Sterols quantification in the serum from SARS-CoV-2 infected and control individuals

The main objective of this observational cohort study was indeed the evaluation of the trend of serum 27OHC concentration in hospitalized moderate and severe COVID-19 patients as well as in PACP versus a control group, but a prior overall look at cholesterol metabolism was deemed essential. Of note, serum concentration of cholesterol and precursor sterols lanosterol, desmosterol (Bloch pathway of cholesterol synthesis) and lathosterol (Kandutsch-Russell pathway of cholesterol synthesis) were all significantly reduced in both moderate and severe COVID-19 patients in comparison to controls ($P < 0.001$) (Fig. 4 and Table S1).

The PACP group showed a cholesterol metabolism picture quite similar to that of the control group, with just a modest but significant reduction in cholesterol and lanosterol serum levels (Fig. 4).

Table 1
Antiviral activity of 2HP-βCD:27OHC.

ID	Virus	EC50[a] (μM) – 95% C.I.[b]	EC90[c] (μM) – 95% C.I.	CC50[d] (μM) – 95% C.I.	SI[e]
2HP-βCD:27OHC	SARS-CoV-2	1.4 (1.1–1.9)	4.0 (2.1–7.6)	364.5 (258.2–572.8)	260.4
	CoV-OC43	1.6 (1.1–2.3)	6.6 (3.0–14.4)	188.5 (123.2–288.5)	117.8
	RSV	n.a.	n.a.	>1350	n.a.
2HP-βCD	SARS-CoV-2	n.a.	n.a.	170.1 (136.8–211.7)	n.a.
	CoV-OC43	n.a	n.a.	>1350	n.a.
	RSV	n.a.	n.a.	>1350	n.a.

n.a. not assessable.
27OHC: 27-hydroxycholesterol.
[a] EC_{50} half-maximal effective concentration.
[b] CI confidence interval.
[c] EC_{90}90% effective concentration.
[d] CC_{50} half maximal cytotoxic concentration.
[e] SI selectivity index.

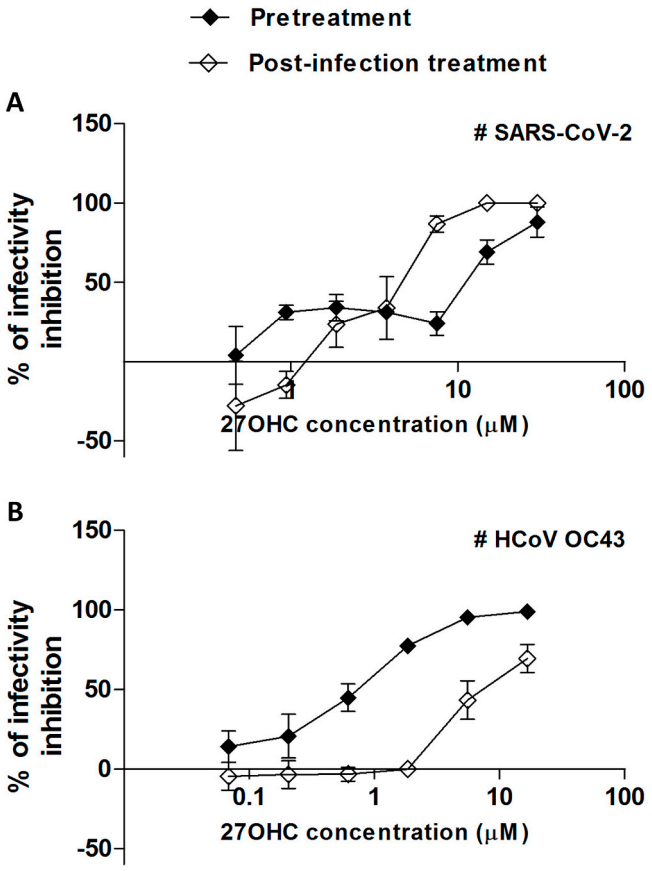

Fig. 2. Time-of-addition experiments. The step of SARS-CoV-2 (A) and HCoV OC43 (B) replicative cycle inhibited by 2HP-βCD:27OHC was investigated. Time-of-addition experiments were performed by treating cells before or after viral inoculum (named respectively "pretreatment" and "post-infection treatment" protocols). The percentage of infectivity inhibition was calculated by comparing the number of viral plaques in treated and untreated wells. Error bars represent the SEM of 2 independent experiments.

3.4. Oxysterols quantification in the serum from COVID-19 patients, PACP and control individuals

By far, the most interesting finding of the cohort study was the marked reduction of serum 27OHC in both moderate and severe COVID-19 patients compared to controls ($P < 0.001$ for both) (Fig. 5 and Table S1).

Actually, the serum 27OHC was already significantly reduced in the PACP group, the mean 27OHC decrease being of 17% in PACP group, 30% in the moderate and of 50% in the severe COVID-19 group (Fig. 5). The PACP group was in between controls and COVID groups (Fig. 5 and Table S1). With regard to the other side chain oxysterols physiologically present in human blood, namely 24OHC and 25OHC, only a slight but significant decrease was observed in all three groups of infected subjects, with the only exception of a modest but significant increase of 25OHC in the PACP group. No correlation at all was observed between 24OHC and 25OHC serum levels and the severity of the disease.

Opposite to that of side chain oxysterols was the behaviour in COVID-19 shown by the two B-ring non enzymatic oxysterols of major pathological meaning, namely 7βOHC and 7KC, actually recognized markers of oxidative stress [25,26]. Serum concentration of both oxysterols showed a significant while moderate increment in severe COVID-19 patients as respect to controls ($P < 0.001$ for both). Serum 7KC but not 7βOHC was significantly increased in the moderate COVID-19 patients as well ($P = 0.002$). In the SARS-CoV-2 positive but pauci- or a-symptomatic subjects, both markers of oxidative stress did not show any significant difference when compared to the control individuals (Fig. 6).

Table 2
Time-of-addition experiments with 2HP-βCD:27OHC.

Virus	Protocol	EC50[a] (μM) – 95% C.I.[b]	EC90[c] (μM) – 95% C.I.
CoV-OC43	pretreatment	0.7 (0.5–1.0)	4.6 (1.9–11.2)
	post-infection treatment	8.3 (5.7–12.1)	34.6 (13.8–86.7)
SARS-CoV-2	pretreatment	7.8 (4.4–13.8)	123.4 (24.2–628.9)
	post-infection treatment	4.3 (3.0–6.2)	9.2 (4.0–21.0)

n.a. not assessable.
[a] EC_{50} half-maximal effective concentration.
[b] CI confidence interval.
[c] EC_{90}90% effective concentration.

4. Discussion

The data reported in this study demonstrate that 27OHC blocks the replication in vitro of two human CoVs belonging to the β-coronavirus genus: SARS-CoV-2 and HCoV-OC43. These findings further confirm the broad spectrum of antiviral activity of 27OHC, which has been already demonstrated for herpes simplex virus, rhinovirus, rotavirus and papillomavirus [5]. Since all of these viruses are phylogenetically unrelated, with ample diversity in their replicative cycles and structures, it is unlikely that 27OHC targets specific functions such as viral enzymes or anti-receptors. Moreover, 27OHC does not directly inactivate the viral particle as shown also in previous studies [8] (Fig. S1). The ability to

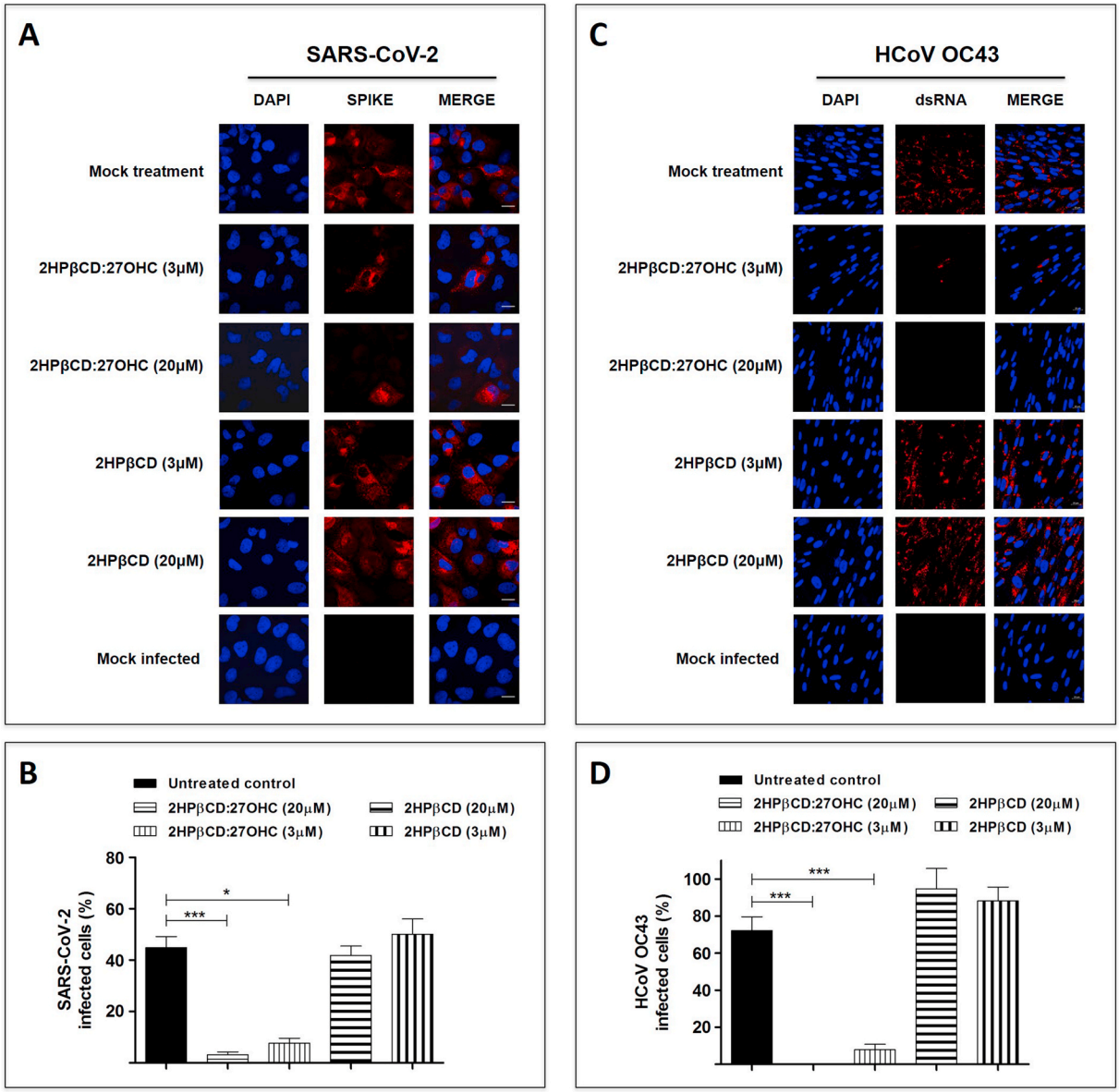

Fig. 3. Infectivity inhibition as assessed by immunofluorescence experiments. Huh-7 (A) and MRC-5(C) cells were infected with SARS-CoV-2 and HCoV OC43 in the presence of 2HP-βCD:27OHC, then fixed at 48 h post-infection and stained with DAPI and specific antibodies. Panels B and D show respectively the number of SARS-CoV-2 and HCoV OC43 positive cells. On the *y* axis, this value is expressed as % of the virus positive cells as compared to DAPI positive cells. Error bars represent the SEM of 2 independent experiments.

impair viral entry and/or replication when added up to 24 h before virus inoculum supports the idea that 27OHC modifies cell structures rather than targeting viral components. Indeed, the host-targeting antiviral mode of action has already been reported by Civra et al. [10], showing that 27OHC induces accumulation of cholesterol in the late endosomal compartment resulting in sequestering human rotavirus particles inside these vesicles, thereby preventing cytoplasmic viral replication. Since also CoVs entry into the host cells involves the endocytic pathway [27–29], the *anti*-CoVs activity of 27OHC appears due, at least in part, to the transient modification of the endosomal membrane composition and function exerted by the oxysterol.

This is especially true in case of 27OHC externally added to the cells, that is in a pharmaceutical mode, in other words as a drug product. Exogenously added 27OHC was proven to almost exclusively accumulate in lipid rafts, as opposed to oxysterols of not enzymatic origin that randomly localize in plasma membranes [12]. Thus, 27OHC is modifying structure and most likely function of these crucial membrane lipid-protein clusters, where by the way the ACE-2 receptor exploited by SARS-CoV-2 to enter the target cells is located [30], and it certainly induces a modification of multivesicular endosome biogenesis, that by lipid rafts is regulated [31]. Further, we very recently observed in HeLa cells a significant 27OHC-dependent down-regulation of cation independent isoform of mannose-6-phosphate receptor (MPRci) [11], a transporter located at late endosomes whose activity appears crucial for all viruses exploiting the endosomal way to enter and diffuse within cells [32–34]. All together, these facts and findings point to the inhibition of virus entry as the primary protective mechanism of 27OHC externally added to cells.

In this relation, very likely appears the involvement of redox reactions at the 27OHC concentration range proven to inhibit SARS-CoV-2 and CoV-OC43 replication, since similar oxysterol's amounts have been previously demonstrated to transiently increase the level of oxidant species in human promonocytic cells through the activation of NADPH oxidase and the modulation of mitochondrial membrane potential [35].

Table 3
Laboratory parameters of hospitalized COVID-19 patients.

Parameter (normal range values)	COVID-19 moderate, n = 36		COVID-19 severe, n = 81		Mann-Withney *U* test
	Mean ± SD	Median IQR Min-Max	Mean ± SD	Median IQR Min-Max	
RBC (4.5–6.5 x 10^9/L)	4.28 ± 0.65	4.39 3.80–4.76 2.67–5.67	4.03 ± 0.69	4.06 3.60–4.46 2.02–6.66	0.07
HB (13–18 mg/dL)	12.61 ± 2.14	13.15 11.05–14.05 7.80–16.70	12.06 ± 2.81	12.00 10.78–13.30 6.70–31.10	0.04
HTC (40–54%)	36.94 ± 6.27	36.50 33.35–41.90 20.80–50.90	34.45 ± 4.65	35.50 31.75–37.50 19.50–44.30	0.04
WBC (4–11 x 10^9/L)	12.35 ± 20.16	7.95 5.85–11.15 2.90–127.00	8.69 ± 4.26	7.70 5.53–11.40 3.50–22.40	0.48
PLT (140–450 x 10^9/L)	262.61 ± 117.17	235.50 171.50–350.00 18.00–525.00	253.51 ± 121.43	231.00 174.75–306.50 13.00–580.00	0.73
NEUT (1.2–6.93 x 10^9/L)	8.20 ± 6.71	5.70 3.85–10.54 1.29–30.62	6.91 ± 4.16	5.46 3.90–9.53 1.67–20.61	0.73
EOS (0–0.37 x 10^9/L)	0.04 ± 0.07	0.00 0.00–0.05 0.00–0.25	0.04 ± 0.09	0.00 0.00–0.04 0.00–0.60	0.86
BASO (0–0.1 x 109/L)	0.00 ± 0.03	0.00 0.00–0.00 0.00–0.13	0.02 ± 0.05	0.00 0.00–0.00 0.00–0.35	0.12
LYMP (0.85–3.23 x 10^9/L	0.89 ± 0.41	0.81 0.69–0.96 0.30–2.20	1.03 ± 0.77	0.82 0.57–1.20 0.17–4.80	0.86
MONO (0–0.67 x 10^9/L)	0.70 ± 0.54	0.48 0.34–0.91 0.08–2.52	0.47 ± 0.28	0.42 0.26–0.62 0.10–1.62	0.05
N/L	10.81 ± 11.18	8.10 5.12–10.99 1.34–47.56	10.94 ± 12.11	7.80 3.63–14.35 0.84–83.94	0.92
CREA (0.5–1.2 mg/dL)	1.45 ± 2.16	0.91 0.80–1.14 0.60–13.35	1.55 ± 1.52	1.14 0.85–1.52 0.35–8.11	0.03
ALT (9–59 U/L)	93.20 ± 141.99	52.00 32.00–99.00 16.00–780.00	74.05 ± 153.77	36.00 24.50–63.50 13.00–1206	0.10
CK (38–174 U/L)	763.73 ± 2438.05	115.00 61.50–180.00 14.00–9565.00	401.84 ± 788.81	156.00 68.00–302.00 9.00–4397	0.35
LDH (125–220 U/L)	369.48 ± 122.89	353.00 280.25–465.50 142.00–620.00	374.07 ± 143.08	347.50 289.50–411.50 171.00–1108	0.88
PCT (0–0.5 ng/mL)	0.44 ± 0.50	0.30 0.16–0.49 0.04–2.24	1.77 ± 5.60	0.27 0.10–0.63 0.03–38.39	0.79
CRP (0.0–5.0 mg/L)	108.48 ± 83.28	91.84 52.38–146.59 4.79–330.79	116.07 ± 87.46	97.60 44.94–162.31 4.22–377.10	0.69

Data are presented as Mean ± SD and as Median, interquartile range IQR, Min-Max.
Red Blood Cells, RBC; Haemoglobin, Hb; Haematocrit (Hct); White Blood Cells, WBC; Platelet Count, PLT; Neutrophil count, NEUT; Eosinophil count, EOS; Basophil count, BASO; Lymphocyte count, LYMP; Monocyte count, MONO; neutrophils/lymphocyte ratio, N/L; creatinine, CREA; alanine aminotranspherase ALT; creatinine-chinase, CK; lactic dehydrogenase, LDH; procalcitonin, PCT; C reactive protein, CRP.

How such a transient oxidative imbalance exerted by 27OHC contributes to its *anti*-SARS-CoV-2 and *anti*-CoV-OC43 activity is matter of ongoing studies, that are also considering this oxysterol ability to induce autophagy [36], a cellular degradation process in principle favouring the elimination of viral pathogens by delivering viral particles for lysosomal degradation and closely interacting with innate immunity [37]. Notably, the pro-autophagic effect of 27OHC observed in human promonocytic cells was abolished by cell pretratment with a selective NADPH oxidase inhibitor [36].

27OHC has also been shown to modulate the immune-response to infections by increasing the expression of dendritic cell markers and MHC classes I and II molecules [38,39] or by activating the TLR4/NF-κB signaling pathway [40], or to induce expression, synthesis and release of Heat Shock Protein 60 (HSP60) [41], a chaperone molecule of mitochondrial origin, recognized to play an important role in the intercellular immune network [42]. Finally, all immune cells express the oxysterols' receptors Liver X (LXRs) [43], but how their activity could be modulated by molecules like 27OHC still has to be elucidated.

The physiological nature of 27OHC and its potential role as first line constitutive effector of the antiviral defences of human body prompted us to analyse the 27OHC serum levels in COVID-19 patients at different stages of disease progression.

Standard laboratory findings achieved in hospitalized patients were consistent with previous reports on COVID-19 [44–47]. Of particular interest were the low or very low serum cholesterol levels observed in moderate and severe COVID-19 patients, respectively (Fig. 4 and Table S1), indicating a severe impairment of cholesterol metabolism. Serum cholesterol has just been shown to be significantly decreased in

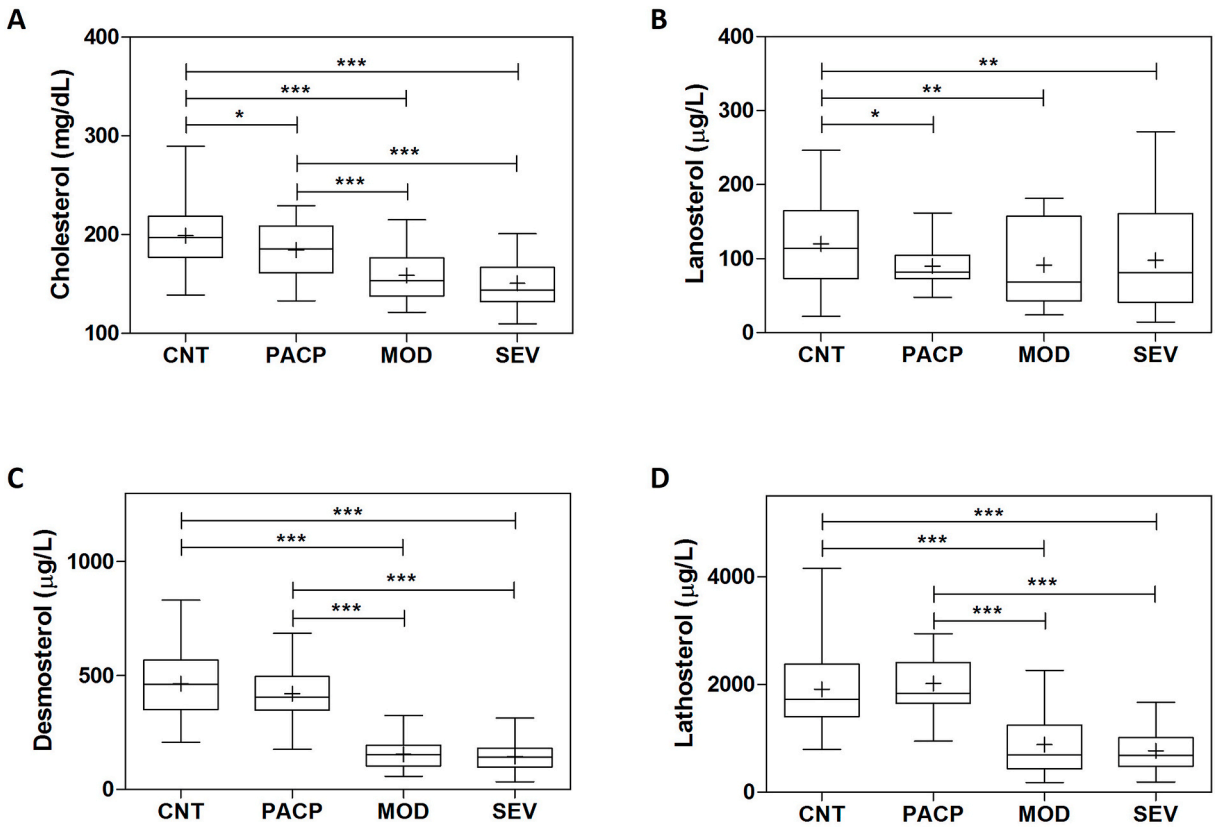

Fig. 4. Serum content of cholesterol and main precursor sterols in SARS-CoV-2 infected subjects. CNT (n = 123): controls; PACP (n = 27): pauci-/a-symptomatic; MOD (n = 36): moderate-COVID-19 patients; SEV (n = 81): severe COVID-19 patients. Mann-Withney *U* test, *P < 0.05; **P < 0.01; ***P < 0.001 (also see Supplementary Table 1).

COVID-19 patients in direct relation with the severity of the disease, with data highly consistent with those obtained in this study [48], while the reduction of the main sterol precursors of cholesterol in COVID-19 has not been reported in the literature yet. A big impairment of cholesterol metabolism, at least in severe COVID-19 patients, was actually expected since a net reduction of cholesterol biosynthesis was described as associated with massive acute phase reaction [49]. Certainly remarkable is the fact that, despite such a profound derangement of cholesterol metabolism in COVID-19, of the three cholesterol oxidation products of enzymatic origin physiologically present in human blood, i.e. 24OHC, 25OHC and 27OHC, only 27OHC showed a pronounced decrease whose intensity tightly correlated to the disease progression (Fig. 5).

The drop in 27OHC serum concentration appeared to be a specific event, since 24OHC was slightly reduced only in moderate (P = 0.036) and severe (P = 0.029) COVID-19 cases, while 25OHC exhibited a small but significant decline only in severe patients (P = 0.018) and it was even slightly increased in the PACP group (P = 0.033 compared to controls, P < 0.001 compared to severe COVID-19 patients), possibly as a consequence of a transiently beneficial INFγ-mediated induction of cholesterol-25-hydroxylase (Fig. 5) [6,50].

Still with regard to the quantification of oxysterols in SARS-CoV-2 infected subjects, a consistent while moderate increase of serum 7-keto-cholesterol and 7β-cholesterol, recognized in vivo markers of oxidative stress, was observed in COVID-19 patients but not in pauci- and a-symptomatic individuals. Actually, an expected finding, because of the serious inflammatory state afflicting those patients, but, to our knowledge, a not yet reported observation.

It is not easy, at present, to identify the reason for the detected selective drop in the 27OHC serum level during SARS-CoV-2 infection in the course of COVID-19. The most plausible hypothesis is that a progressive "mitochondrial stress" would occur at systemic level in those pathological conditions, and that such an impairment would affect the activity of the ubiquitous mitochondrial 27-cholesterol hydroxylase (Cyp27A1) [51], which is the enzyme that converts cholesterol to 27OHC.

Whatever is the actual cause of the progressive reduction of 27OHC in the course of COVID-19, this observational clinical study definitely suggests the opportunity of counteracting such an event, in order to reinforce or reintegrate the antiviral defence system with the administration of suitably formulated 27OHC endowed with antiviral activity.

Notably, the inhibitory activity also shown against CoV-OC43, which is responsible for 10–20% of the cases of common cold together with CoV-229E [52], further highlights the broad antiviral effect of 27OHC, thus opening interesting perspectives on its consideration in future strategies against emerging coronaviruses.

5. Conclusions

In conclusion, this report demonstrates the antiviral activity of 27OHC against SARS-Cov-2 and one related β-coronavirus and shows the dramatic decrease of physiological levels of 27OHC in severe COVID-19. Although the latter observation deserves further investigation, the identification of 27OHC as a novel physiological antiviral with a broad spectrum against β-coronaviruses may be of great importance for the treatment of SARS-CoV-2 infections and possible future epidemics.

Declaration of interests

Andrea Civra, David Lembo, Giuseppe Poli are the founders of Panoxyvir Ltd., a start-up developing the use of specific oxysterols as broad antiviral agents. Panoxyvir Ltd., together with ICGEB, the affiliation of

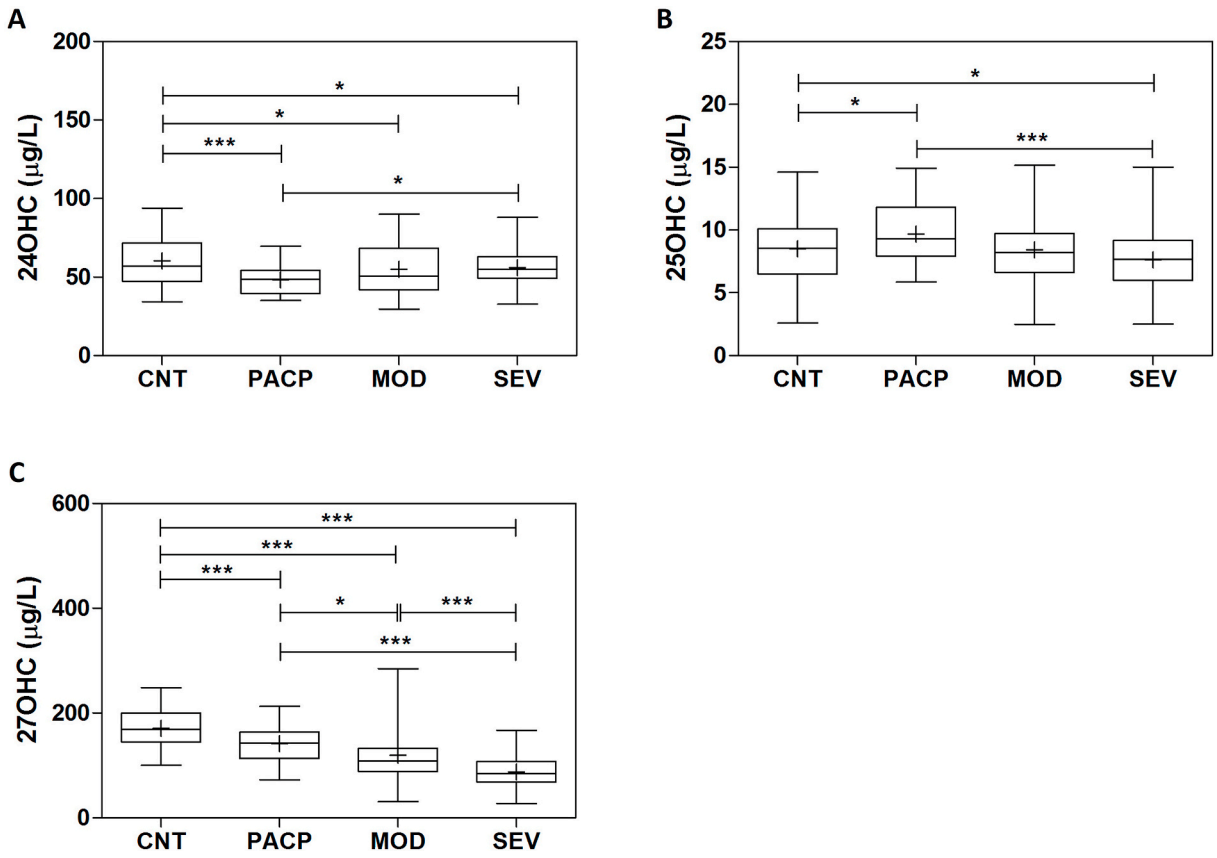

Fig. 5. Serum concentration of side-chain oxysterols 24OHC, 25OHC, 27OHC in SARS-CoV-2 infected subjects. CNT (n = 123): controls; PACP (n = 27): pauci-/a-symptomatic; MOD (n = 36): moderate-COVID-19 patients; SEV (n = 81): severe COVID-19 patients. Mann-Withney *U* test, *P < 0.05; **P < 0.01; ***P < 0.001 (also see Supplementary Table 1).

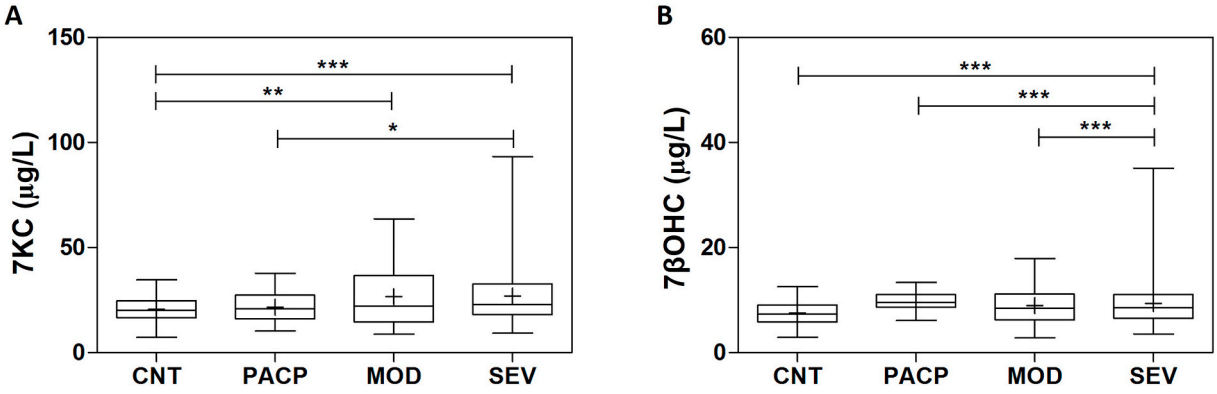

Fig. 6. Serum level of 7KC and 7βOHC in SARS-CoV-2 positive subjects. CNT (n = 123): controls; PACP (n = 27): pauci-/a-symptomatic; MOD (n = 36): moderate-COVID-19 patients; SEV (n = 81): severe COVID-19 patients. Mann-Withney *U* test, *P < 0.05; **P < 0.01; ***P < 0.001 (also see Supplementary Table 1).

the fourth inventor Alessandro Marcello, filed on April 2020 an application to patent the use of 27-hydroxycholesterol in the treatment and/or prevention of diseases caused by Coronaviruses (app n. 102020000008977). Panoxyvir did not provide any financial support to this study. All authors declare no other competing financial interests or conflicts of interest.

Author contributions

Conceptualization, D.L., G.P., and V.L.; Methodology, A.M., V.L., S. R., M.A., R.C.; Investigation, A.M., A.C., V.L., R.B., L.A.N., C.G., C.C., R. C.; Writing – Original Draft, G.P., V.L., D.L.; Writing – Review & Editing, A.M., D.L., V.L., A.C., and G.P.; Funding Acquisition, A.M., D.L.; Resources, P.B., C.G., M.A.; Supervision, A.M, D.L., V.L.; Project administration: D.L. and G.P.

Acknowledgements

The authors gratefully acknowledge Dr. Rosanna Falbo, Laboratory of Clinical Chemistry, Hospital of Desio, ASST-Monza, for linguistic revision of the manuscript. This work was supported by Beneficentia Stiftung, Vaduz, Liechtenstein and SNAM Foundation, San Donato Milanese, Milan, Italy (grants to A.M.), by the University of Turin, Italy (grant RILO19 and LEMB_RIC_COMP_20_01 to D.L.), by CRT

Foundation, Turin, Italy (grant CIVA_CRT_20_01 to A.C.).

Appendix A. Supplementary data

Supplementary data to this article can be found online at https://doi.org/10.1016/j.redox.2020.101682.

References

[1] J.M. Sanders, M.L. Monogue, T.Z. Jodlowski, J.B. Cutrell, Pharmacologic treatments for coronavirus disease 2019 (COVID-19): a review, J. Am. Med. Assoc. 323 (2020) 1824–1836, https://doi.org/10.1001/jama.2020.6019.

[2] M.K. Zakaria, T. Carletti, A. Marcello, Cellular targets for the treatment of Flavivirus infections, Front. Cell. Infect. Microbiol. 8 (2018) 398, https://doi.org/10.3389/fcimb.2018.00398.

[3] S.J. Bensinger, P. Tontonoz, Integration of metabolism and inflammation by lipid-activated nuclear receptors, Nature 454 (2008) 470–477, https://doi.org/10.1038/nature07202.

[4] S.J. Bensinger, M.N. Bradley, S.B. Joseph, N. Zelcer, E.M. Janssen, M.A. Hausner, R. Shih, J.S. Parks, P.A. Edwards, B.D. Jamieson, P. Tontonoz, LXR signaling couples sterol metabolism to proliferation in the acquired immune response, Cell 134 (2008) 97–111, https://doi.org/10.1016/j.cell.2008.04.052.

[5] D. Lembo, V. Cagno, A. Civra, G. Poli, Oxysterols: an emerging class of broad spectrum antiviral effectors, Mol. Aspect. Med. 49 (2016) 23–30.

[6] S.Y. Liu, R. Aliyari, K. Chikere, G. Li, M.D. Marsden, J.K. Smith, O. Pernet, H. Guo, R. Nusbaum, J.A. Zack, A.N. Freiberg, L. Su, B. Lee, G. Cheng, Interferon-inducible cholesterol-25-hydroxylase broadly inhibits viral entry by production of 25-hydroxycholesterol, Immunity 38 (2013) 92–105.

[7] C. Li, Y.-Q. Deng, S. Wang, F. Ma, R. Aliyari, X.-Y. Huang, N.-N. Zhang, M. Watanabe, H.-L. Dong, P. Liu, X.-F. Li, Q. Ye, M. Tian, S. Hong, J. Fan, H. Zhao, L. Li, N. Vishlaghi, J.E. Buth, C. Au, Y. Liu, N. Lu, P. Du, F.X.-F. Qin, B. Zhang, D. Gong, X. Dai, R. Sun, B.G. Novitch, Z. Xu, C.-F. Qin, G. Cheng, 25-Hydroxycholesterol protects host against Zika virus infection and its associated microcephaly in a mouse model, Immunity 46 (2017) 446–456, https://doi.org/10.1016/j.immuni.2017.02.012.

[8] A. Civra, V. Cagno, M. Donalisio, F. Biasi, G. Leonarduzzi, G. Poli, D. Lembo, Inhibition of pathogenic non-enveloped viruses by 25-hydroxycholesterol and 27-hydroxycholesterol, Sci. Rep. 4 (2014) 7487.

[9] V. Cagno, A. Civra, D. Rossin, S. Calfapietra, C. Caccia, V. Leoni, N. Dorma, F. Biasi, G. Poli, D. Lembo, Inhibition of herpes simplex-1 virus replication by 25-hydroxycholesteroland 27-hydroxycholesterol, Redox. Biol. 12 (2017) 522–527.

[10] A. Civra, R. Francese, P. Gamba, G. Testa, V. Cagno, G.G. Poli, D. Lembo, 25-Hydroxycholesterol and 27-hydroxycholesterol inhibit human rotavirus infection by sequestering viral particles into late endosomes, Redox. Biol. 19 (2018) 318–330, https://doi.org/10.1016/j.redox.2018.09.003.

[11] A. Civra, M. Colzani, V. Cagno, R. Francese, V. Leoni, G. Aldini, D. Lembo, G. Poli, Modulation of cell proteome by 25-hydroxycholesterol and 27-hydroxycholesterol: a link between cholesterol metabolism and antiviral defense, Free Radic. Biol. Med. 149 (2020) 30–36, https://doi.org/10.1016/j.freeradbiomed.2019.08.031.

[12] K. Ragot, J.J. Mackrill, A. Zarrouk, T. Nury, V. Aires, A. Jacquin, A. Athias, J. P. Pais de Barros, A. Véjux, J.M. Riedinger, D. Delmas, G. Lizard, Absence of correlation between oxysterol accumulation in lipid raft microdomains, calcium increase, and apoptosis induction on 158N murine oligodendrocytes, Biochem. Pharmacol. 86 (2013) 67–79, https://doi.org/10.1016/j.bcp.2013.02.028.

[13] S. Dambal, M. Alfaqih, S. Sanders, E. Maravilla, A. Ramirez-Torres, G.C. Galvan, M. Reis-Sobreiro, M. Rotinen, L.M. Driver, M.S. Behrove, T. Jovanovic Talisman, J. Soon, S. You, J. Turkson, J.-T. Chi, M.R. Freeman, E. Macias, S.J. Freedland, 27-Hydroxycholesterol impairs plasma membrane lipid raft signaling as evidenced by inhibition of IL6-JAK-STAT3 signaling in prostate cancer cells, Mol. Canc. Res. 18 (2020) 671–684, https://doi.org/10.1158/1541-7786.MCR-19-0974.

[14] V. Leoni, C. Caccia, Oxysterols as biomarkers in neurodegenerative diseases, Chem. Phys. Lipids 164 (2011) 515–524, https://doi.org/10.1016/j.chemphyslip.2011.04.002.

[15] I. Björkhem, V. Leoni, S. Meaney, Genetic connections between neurological disorders and cholesterol metabolism, J. Lipid Res. 51 (2010) 2489–2503, https://doi.org/10.1194/jlr.R006338.

[16] A. Civra, V. Leoni, C. Caccia, S. Sottemano, P. Tonetto, A. Coscia, C. Peila, G. E. Moro, P. Gaglioti, E. Bertino, G. Poli, D. Lembo, Antiviral oxysterols are present in human milk at diverse stages of lactation, J. Steroid Biochem. Mol. Biol. 193 (2019) 105424, https://doi.org/10.1016/j.jsbmb.2019.105424.

[17] S. Rajasekharan, R.M. Bonotto, Y. Kazungu, L.N. Alves, M. Poggianella, P. Martinez Orellana, N. Skoko, S. Polez, A. Marcello, Repurposing of Miglustat to Inhibit the Coronavirus Severe Acquired Respiratory Syndrome SARS-CoV-2. BioRxiv 2020 preprint. doi: 10.1101/2020.05.18.101691.

[18] D. Licastro, S. Rajasekharan, S. Dal Monego, L. Segat, P. D'Agaro, A. Marcello, Isolation and full-length genome characterization of SARS-CoV-2 from COVID-19 cases in northern Italy, J. Virol. 94 (2020), https://doi.org/10.1128/JVI.00543-20 e0054.3-20.

[19] V. Cagno, M. Donalisio, A. Civra, M. Volante, E. Veccelli, P. Oreste, M. Rusnati, D. Lembo, Highly sulfated K5 Escherichia Coli polysaccharide derivatives inhibit respiratory syncytial virus infectivity in cell lines and human tracheal-bronchial histocultures, Antimicrob. Agents Chemother. 58 (2014) 4782–4794, https://doi.org/10.1128/AAC.02594-14.

[20] Y. Deng, W. Liu, K. Liu, Y.Y. Fang, J. Shang, L. Zhou, K. Wang, F. Leng, S. Wei, L. Chen, H.G. Liu, Clinical characteristics of fatal and recovered cases of coronavirus disease 2019 in Wuhan, China: a retrospective study, Chin. Med. J. 133 (2020) 1261–1267, https://doi.org/10.1097/CM9.0000000000000824.

[21] Y. Gao, T. Li, M. Han, X. Li, D. Wu, Y.Y. Xu, Zhu, Y. Liu, X. Wang, L. Wang, Diagnostic utility of clinical laboratory data determinations for patients with the severe COVID-19, J. Med. Virol. 92 (2020) 791–796, https://doi.org/10.1002/jmv.25770.

[22] S. Tian, N. Hu, J. Lou, K. Chen, X. Kang, Z. Xiang, H. Chen, D. Wang, N. Liu, D. Liu, G. Chen, Y. Zhang, D. Li, J. Li, H. Lian, S. Niu, L. Zhang, J. Zhang, Characteristics of COVID-19 infection in Beijing, J. Infect. 80 (2020) 401–406, https://doi.org/10.1016/j.jinf.2020.02.018.

[23] F. Zhou, T. Yu, R. Du, G. Fan, Y. Liu, Z. Liu, J. Xiang, Y. Wang, B. Song, X. Gu, L. Guan, Y. Wei, H. Li, X. Wu, J. Xu, S. Tu, Y. Zhang, H. Chen, B. Cao, Clinical course and risk factors for mortality of adult inpatients with COVID-19 in Wuhan, China: a retrospective cohort study, Lancet 395 (10229) (2020) 1054–1062, https://doi.org/10.1016/S0140-6736(20)30566-3.

[24] Z. Wu, J.M. McGoogan, Characteristics of and important lessons from the coronavirus disease 2019 (COVID-19) outbreak in China: summary of a report of 72 314 cases from the Chinese center for disease control and prevention, JAMA Feb 24 (2020), https://doi.org/10.1001/jama.2020.2648.

[25] M. Arca, S. Natoli, F. Micheletta, S. Riggi, E. Di Angelantonio, A. Montali, T. M. Antonini, R. Antonini, U. Diczfalusy, L. Iuliano, Increased plasma levels of oxysterols, in vivo markers of oxidative stress, in patients with familial combined hyperlipidemia: reduction during atorvastatin and fenofibrate therapy, Free Radic. Biol. Med. 42 (2007) 698–705, https://doi.org/10.1016/j.freeradbiomed.2006.12.013.

[26] C. Zerbinati, L. Iuliano, Cholesterol and related sterols autoxidation, Free Radic. Biol. Med. 111 (2017) 151–155, https://doi.org/10.1016/j.freeradbiomed.2017.04.013.

[27] Y. Inoue, N. Tanaka, Y. Tanaka, S. Inoue, K. Morita, M. Zhuang, T. Hattori, K. Sugamura, Clathrin-dependent entry of severe acute respiratory syndrome coronavirus into target cells expressing ACE2 with the cytoplasmic tail deleted, J. Virol. 81 (2007) 8722–8729, https://doi.org/10.1128/JVI.00253-07.

[28] H. Wang, P. Yang, K. Liu, F. Guo, Y. Zhang, G. Zhang, C. Jiang, SARS coronavirus entry into host cells through a novel clathrin- and caveolae-independent endocytic pathway, Cell Res. 18 (2008) 290–301, https://doi.org/10.1038/cr.2008.15.

[29] T. Tang, M. Bidon, J.A. Jaimes, G.R. Whittaker, S. Daniel, Coronavirus membrane fusion mechanism offers a potential target for antiviral development, Antivir. Res. 178 (2020) 104792, https://doi.org/10.1016/j.antiviral.2020.104792.

[30] Y. Lu, D.X. Liu, J.P. Tam, Lipid rafts are involved in SARS-CoV entry into Vero E6 cells, Biohcim. Biophys. Res. Communs. 369 (2008) 344–349, https://doi.org/10.1016/j.bbrc.2008.02.023.

[31] C. Bissig, J. Gruenberg, Lipid sorting and multivesicular endosome biogenesis, Cold Spring Harb. Perspect. Biol. 5 (2013) a016816, https://doi.org/10.1101/cshperspect.a016816.

[32] M. Gary-Bobo, P. Nirdé, A. Jeanjean, A. Morère, M. Garcia, Mannose 6-phosphate receptor targeting and its applications in human diseases, Curr. Med. Chem. 14 (2007) 2945–2953, https://doi.org/10.2174/092986707782794005.

[33] Y. Chen, K.M. Honeychurch, G. Yang, C.M. Byrd, C. Harver, D.E. Hruby, R. Jordan, Vaccinia virus p37 interacts with host proteins associated with LE-derived transport vesicle biogenesis, Virol. J. 6 (2009) 44, https://doi.org/10.1186/1743-422X-6-44.

[34] M.A. Díaz-Salinas, L.A. Casorla, T. López, S. López, C.F. Arias, Most rotavirus strains require the cation-independent mannose-6-phosphate receptor, sortilin-1, and cathepsins to enter cells, Virus Res. 245 (2018) 44–51, https://doi.org/10.1016/j.virusres.2017.12.002.

[35] B. Vurusaner, P. Gamba, G. Testa, S. Gargiulo, F. Biasi, C. Zerbinati, L. Iuliano, G. Leonarduzzi, H. Basaga, G. Poli, Survival signaling elicited by 27-hydroxycholesterol through the combined modulation of cellular redox state and ERK/Akt phosphorylation, Free Radic. Biol. Med. 77 (2014) 376–385, https://doi.org/10.1016/j.freeradbiomed.2014.07.026.

[36] B. Vurusaner, S. Gargiulo, G. Testa, P. Gamba, G. Leonarduzzi, G. Poli, H. Basaga, The role of autophagy in survival response induced by 27-hydroxycholesterol in human promonocytic cells, Redox. Biol. 17 (2018) 400–410, https://doi.org/10.1016/j.redox.2018.05.010.

[37] Y. Tian, M.-L. Wang, J. Zhao, Crosstalk between autophagy and type I interferon responses in innate antiviral immunity, Viruses 11 (2019) 132, https://doi.org/10.3390/v11020132.

[38] Y. Son, S.-M. Kim, S.-A. Lee, S.-K. Eo, K. Kim, Oxysterols induce transition of monocytic cells to phenotypically mature dendritic cell-like cells, Biochem. Biophys. Res. Commun. 438 (2013) 161–168, https://doi.org/10.1016/j.bbrc.2013.07.046.

[39] Y. Son, J. Choi, B. Kim, Y.C. Park, S.-K. Eo, H.R. Cho, S.S. Bae, C.D. Kim, K. Kim, Cyclosporin A inhibits differentiation and activation of monocytic cells induced by 27-hydroxycholesterol, Int. Immunopharm. 69 (2019) 358–367, https://doi.org/10.1016/j.intimp.2019.01.045.

[40] S. Gargiulo, P. Gamba, G. Testa, D. Rossin, B. Biasi, G. Poli, G. Leonarduzzi, Relation between TLR4/NF-κB signaling pathway activation by 27-hydroxycholesterol and 4-hydroxynonenal, and atherosclerotic plaque instability, Aging Cell 14 (2015) 569–581, https://doi.org/10.1111/acel.12322.

[41] B.-Y. Kim, Y. Son, J. Choi, S.-K. Eo, Y.C. Park, K. Kim, 27-Hydroxycholesterol upregulates the production of heat shock protein 60 of monocytic cells, J. Steroid Biochem. Mol. Biol. 172 (2017) 29–35, https://doi.org/10.1016/j.jsbmb.2017.04.015.

[42] F. Quintana, I.R. Cohen, Theop HSP60 immune system network, Trends Immunol. 32 (2011) 89–95, https://doi.org/10.1016/j.it.2010.11.001.
[43] Y. Kidani, S.J. Bensinger, LXR and PPAR as integrators of lipid homeostasis and immunity, Immunol. Rev. 249 (2012) 72–83, https://doi.org/10.1111/j.1600-065X.2012.01153.x.
[44] Y. Zhou, Z. Yang, Y. Guo, S. Geng, S. Gao, S. Ye, Y. Hu, Y.Y. Wang, A new predictor of disease severity in patients with COVID-19 in Wuhan, China, medRxiv (2020), https://doi.org/10.1101/2020.03.24.20042119, 2020.03.24.20042119.
[45] G. Lippi, M. Plebani, The critical role of laboratory medicine during coronavirus disease 2019 (COVID-19) and other viral outbreaks, Clin. Chem. Lab. Med. 58 (7) (2020) 1063–1069, https://doi.org/10.1515/cclm-2020-0240.
[46] N. Chen, M. Zhou, X. Dong, J. Qu, F. Gong, Y. Han, Y. Qiu, J. Wang, Y. Liu, Y. Wei, J. Xia, T. Yu, X. Zhang, L. Zhang, Epidemiological and clinical characteristics of 99 cases of 2019 novel coronavirus pneumonia in Wuhan, China: a descriptive study, Lancet 395 (10223) (2020) 507–513, https://doi.org/10.1016/S0140-6736(20)30211-7.
[47] G. Grasselli, A. Zangrillo, A. Zanella, M. Antonelli, L. Cabrini, A. Castelli, D. Cereda, A. Coluccello, G. Foti, R. Fumagalli, G. Iotti, N. Latronico, L. Lorini, S. Merler, G. Natalini, A. Piatti, M.V. Ranieri, A.M. Scandroglio, E. Storti, M. Cecconi, A. Pesenti, COVID-19 Lombardy ICU Network, Baseline characteristics and outcomes of 1591 patients infected with SARS-CoV-2 admitted to ICUs of the Lombardy Region, Italy. JAMA 323 (16) (2020) 1574–1581, https://doi.org/10.1001/jama.2020.5394.
[48] X. Wei, W. Zeng, J. Su, H. Wan, X. Yu, X. Cao, W. Tan, H. Wang, Hypolipidemia is associated with the severity of COVID-19, J. Clin. Lipidol. 14 (2020) 297–304, https://doi.org/10.1016/j.jacl.2020.04.008.
[49] Y.A. Carpentier, O. Scruel, Changes in the concentration and composition of plasma lipoproteins during the acute phase response, Curr. Opin. Clin. Nutr. Metab. Care 5 (2002) 153–158, https://doi.org/10.1097/00075197-200203000-00006.
[50] M. Blanc, W.Y. Hsieh, K.A. Robertson, K.A. Kropp, T. Forster, G. Shui, P. Lacaze, S. Watterson, S.J. Griffiths, N.J. Spann, A. Meljon, S. Talbot, K. Krishnan, D. F. Covey, M.R. Wenk, M. Craigon, Z. Ruzsics, J. Haas, A. Angulo, W.J. Griffiths, C. K. Glass, Y. Wang, P. Ghazal, The transcription factor STAT-1 couples macrophage synthesis of 25-hydroxycholesterol to the interferon antiviral response, Immunity 38 (2013) 106–118.
[51] I. Bjorkhem, Are side-chain oxidized oxysterols regulators also in vivo? J. Lipid Res. 50 (2009) 213–218, https://doi.org/10.1194/jlr.R800025-JLR200. Suppl.S.
[52] T. Heikinnen, A. Järvinen, The common cold, Lancet 361 (2003) 51–59, https://doi.org/10.1016/S0140-6736(03)12162-9.